Experimental Mechanics
https://doi.org/10.1007/s11340-024-01064-y

RESEARCH PAPER

High Speed Impact Testing of UHMWPE Composite Using Orthogonal Arrays

T. Hannah[1] · V. Martin[1] · S. Ellis[2] · R. H. Kraft[3,4]

Received: 7 July 2023 / Accepted: 25 March 2024

Abstract

Background Ultra high molecular weight polyethylene composites are fiber based composites used in armor applications. While some characterization has been conducted experimentally, this study varies multiple parameters simultaneously to investigate material response under a wide range of conditions.

Objective This work focuses on characterizing the response of Dyneema® HB26 hard laminate composites under high-speed impacts to examine the influence of plate diameter, clamping pressure, and plate spacing on target performance. Additionally, micro Computer Tomography scans are used to nondestructively evaluate the damage evolution in the targets.

Methods These scan results are used in concert with more traditional armor performance metrics to evaluate the effect of various parameters using the method of orthogonal array analysis. This technique allows for multiple variables to be investigated in the same test series, saving time and budget while still providing quality results across a range of variables and variable values.

Results We conclude that of the parameters investigated, the plate spacing parameter has the largest effect on performance, followed by the plate diameter. Bolt torque was found to not have a significant impact on results, indicating that an edge clamping pressure is not critical to material response. Additionally, by examining the high resolution scans, we can quantify the damage with an effective damage angle and that this angle is a good predictor of performance.

Conclusion Finally a damage theory involving the effective bending strength of the plates is discussed as an explanation for all of the results observed in this test series.

Keywords Composites · Orthogonal array testing · CT scanning · Composite failure · Impact testing

Introduction

Ultra-high molecular weight polyethylene (UHMWPE) composites are fiber based polymer composites which have grown in popularity as bullet and fragment mitigating armor packages [1–6]. While there has been some experimentation conducted to characterize the responses of the laminate while varying projectile speed or material thickness [1, 7] little work has been done to characterize additional effects such as the impact of various boundary conditions or the effectiveness of multi-plate stacks of the composite relative to a consolidated whole, especially so in a single study [8, 9]. The exact use case of the material, especially when used for light vehicle protection, can include variations in

✉ R. H. Kraft
Rhk12@psu.edu

T. Hannah
Twh5306@psu.edu

V. Martin
Vam140@psu.edu

S. Ellis
ellis@lanl.gov

[1] The Pennsylvania State University, University Park, 336 Leonhard Building, State College PA 16802, USA

[2] Los Alamos National Lab, LANL MS T086, P.O. Box 1663, Los Alamos NM 87544, USA

[3] Dept. of Mechanical Engineering, Co-Hire, Institute for Computational and Data Sciences, The Pennsylvania State University, University Park, 320 Leonhard Building, State College PA 16802, USA

[4] Dept. of Biomedical Engineering, Co-Hire, Institute for Computational and Data Sciences, The Pennsylvania State University, University Park, 320 Leonhard Building, State College PA 16802, USA

Published online: 17 April 2024

deployed configurations involving geometry changes and boundary conditions based on the available volume and protection implementation. These effects have the potential to change the performance of the material, so understanding the relative impact of them becomes critical. In this work, HB26 Dyneema® panels are tested in multiple configurations using the method of orthogonal arrays for test design [10, 11]. This testing structure allows for direct comparisons between a range of configurations including the influence of air gaps, the diameter of the targets, and clamping pressure or in plane boundary conditions. High resolution computer tomography (CT) methods are also employed to non-destructively investigate the interior of targets post test [9, 12]. The CT scans are used to evaluate the change in damage mechanisms across the testing parameters, and a new evaluation metric called the damage angle is proposed as a new metric to quantify the internal damage effected zone of the composite.

Methods and Setup

Test Matrix and Parameter Definitions

The test matrix used in the main battery of tests is shown in Table 1. This testing scheme follows the method of orthogonal arrays, discussed in Appendix A, and reduces from 27 tests to the 9 shown here. The major evaluation criteria will be exit velocity of the penetrator or amount of un-penetrated material ahead of the projectile when there is no full penetration. The target projectile velocity, 1,030 m/s, should be stopped by the 25.4 mm thick plates by design to give an immediate result of performance if there is a penetration of the multi-plate stacks. All of the 25.4 mm thick plates stopped the projectile while all of the multi-plate stacks did not, which helps simplify the analysis in some respects. This will be further addressed in the "Results" section.

Table 1 Orthogonal test matrix for the main experimental series showing the parameters of Plate Diameter, Plate Spacing, and Bolt Torque

Test #	Plate diameter	Plate Spacing	Bolt Torque
1	20.3 cm	one 25.4 mm thick plate	16.3 N-m
2	15.2 cm	two 12.7 mm thick plates	9.5 N-m
3	25.4 cm	four 6.35 mm thick plates	2.7 N-m
4	20.3 cm	two 12.7 mm thick plates	2.7 N-m
5	15.2 cm	four 6.35 mm thick plates	16.3 N-m
6	25.4 cm	one 25.4 mm thick plate	9.5 N-m
7	20.3 cm	four 6.35 mm thick plates	9.5 N-m
8	15.2 cm	one 25.4 mm thick plate	2.7 N-m
9	25.4 cm	two 12.7 mm thick plates	16.3 N-m

The parameters were selected to probe various responses of the material. The plate diameter parameter and bolt torque parameters investigate the impact of the boundary conditions on performance. The diameter relates to the distance from the impact location to the support, described in "Test Fixture Design" section and Appendix B, while the bolt torque variations simulate the effect of semi-free vs fix boundary conditions parallel to the plate face. The spacing parameter is the most novel, weighing the potential benefit of allowing deformation and failure intermittently vs load transmission through the material via the transverse sound speed to spread the load through the material. For the purposes of this study, the gap is held constant for the two and four plate stacks with the gap values based on preliminary testing results. Further details on these parameters and the selection rationale are provided in Appendix A.

Test Fixture Design

Each plate is clamped in a set of aluminum rings which are then mounted to a larger testing frame which is aligned parallel to the axis of the barrel firing the projectile. The alignment is maintained by securing the frame to a rail which is aligned and permanently affixed to the barrel mount. The clamp ring assembly and mounting structure are shown in Fig. 1 and full drawings are provided in Appendix B. Each set of rings is designed such that the outer 16 mm of the plate is secured between them. This leaves an exposed area of 22.2 cm, 17.1 cm, and 12 cm for the three sized plates. Each set of rings is secured together with 12 bolts which are torqued down to the various prescribed values provided in Table 1. In this structure, the gap between any two plates can be set by moving the clamping rings to a desired location and tightening the mounting screws to secure the plate in place. For the 4 plate stacks, the plates are separated by the rings shown on the third page of Appendix B. The assembly is held together by threading bolts through the holes of each ring and threading into the threaded back ring on the second page of Appendix B. This configuration ensures that the gap for each plate in these multi-plate stacks is consistent.

CT Scans

After the experiments are completed, the plates are scanned using a micro CT scanner capable of scanning at voxel resolutions up to 1 um. For these samples, an area of approximately 10 cm by 10 cm was scanned at a resolution of 55.7 um. This provided a good compromise between amount of plate scanned vs resolution for the machine. While this is not fine enough to resolve individual fibers, which measure 17-19 um, it is enough to examine plys and evaluate failure mechanisms such as delamination, fiber breakage, and other meso and macro mechanical mechanisms. To achieve this

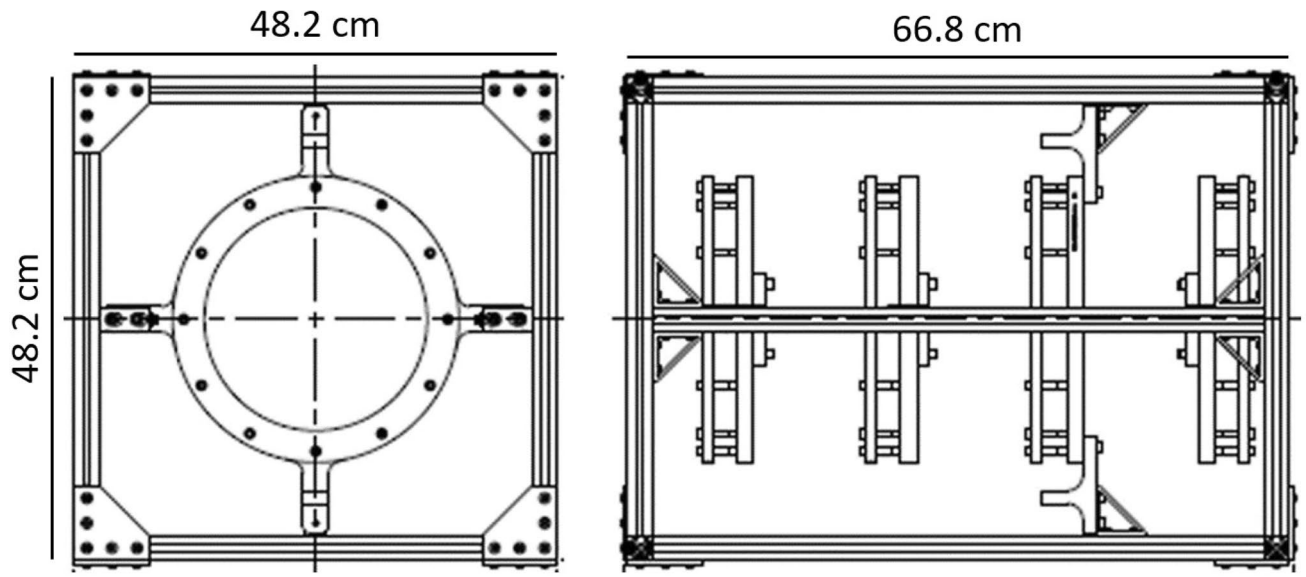

Fig. 1 The plates are clamped between aluminum rings and mounted to a rigid test frame as shown on the left, with potential mount points on the top, bottom, left, and right. The image on the right shows how multiple plates can be inserted into the test frame and gaps can be prescribed at the user's discretion. The full schematics are given in Appendix B

level of resolution the 25.4 cm diameter targets needed to be cut down to 20.3 cm. This is to ensure that the sensor head of the CT could get close enough to the area of interest to maintain spatial resolution. The 25.4 cm samples were cut using a waterjetting process in which the samples were clamped between two sacrificial aluminum rings. The rings both added compressive strength to prevent layer blow-out and reduced the harshness of the cut on the composite by having the initial blast from the jet interact with the sacrificial metal surface first. This resulted in a smooth cut surface with minimal aggregate deposition and no added damage in the specimens. Practice cuts on spare stock were conducted and no delamination or other defects were observed after the cutting. Little to no aggregate or other particulates were seen in the CT scans of these plates, providing additional confidence that the area of interest around the penetration sight was not affected by the cutting process.

Results and Discussion

Calibration Tests

Before the actual experimental specifications were finalized, several calibration shots were run to gather initial data and roughly determine the impact speed to be used for the main series of tests. In these calibration tests it was found that the approximate penetration velocity for the 9.5 mm diameter hardened tool steel projectile was 1100 m/s for the 20.3 cm by 2.54 cm target which was taken as the baseline. During these tests a 15.2 cm by 2.54 cm plate was able to stop a projectile with an initial velocity of 1170 m/s, giving a preliminary insight into the impact of diameter on material behavior being that a smaller diameter leads to increased ballistic performance. From these tests, a target velocity of 1,025–1,035 m/s was selected for the main testing group. This selection helped get an immediate result of the change in performance if the multi-plate stacks were fully penetrated, which indeed they were.

Main Testing Results

The results of the main testing array are shown below in Table 2. All of the consolidated 25.4 mm thick plates stopped the projectile inside the plate. The 15.2 cm diameter plates performed the best with 4.64 mm of unpunctured plate remaining ahead of the projectile, a 53% improvement over the largest 25.4 cm diameter plate of the same thickness and about 14% better than the 20.3 cm diameter plate. While each test did have different bolt torque and therefore clamp pressure, this preliminary assessment aligns with the conclusions from the calibration testing which shows that smaller diameter plates perform better when in this type of testing configuration. Such a result indicates that the interactions with the plate and assembly frame lead to increased performance, as the smaller diameter plate is able to transfer some of the load into the frame faster via the wave speed of the plate compared to larger plates which have a longer travel distance to the assembly frame. The smaller plates also perform better in the multi plate tests, as tests 2 and 5 have two of the lowest exit velocities of the

Table 2 Results of from the main testing including initial penetrator velocity as well as exit velocity for punctured plates and unpunctured plate remaining for non-punctured plates

Test #	Diameter	Plate spacing	Initial Velocity	Exit Velocity / Unpunctured Plate Remaining	delta v
1	20.3 cm	1×25.4 mm	1030 m/s	n/a, 4.09 mm	n/a
2	15.2 cm	2×12.7 mm	1040 m/s	345 m/s	695 m/s
3	25.4 cm	4×6.35 mm	1085 m/s	540 m/s	545 m/s
4	20.3 cm	2×12.7 mm	995 m/s	230 m/s	765 m/s
5	15.2 cm	4×6.35 mm	1020 m/s	310 m/s	710 m/s
6	25.4 cm	1×25.4 mm	1010 m/s	n/a, 4.64 mm	n/a
7	20.3 cm	4×6.35 mm	1015 m/s	515 m/s	500 m/s
8	15.2 cm	1×25.4 mm	1060 m/s	n/a, 3.03 mm	n/a
9	25.4 cm	2×12.7 mm	1040 m/s	425 m/s	615 m/s

two and four plate stacks respectively with 345 m/s for the two plate and 310 m/s for the four plate configurations. Test 4 involving two 20.3 cm plates did have the lowest exit velocity, but it also had the lowest initial velocity by about 20 m/s compared to the next lowest and 35 m/s below the target velocity which should in part account for the perceived increased performance. This decrease is due to the projectile slightly nicking the sabot catcher on the way to the target, which slightly altered its trajectory and decreased its impact velocity. However, the impact velocity is still high enough to consider this data point with the caveat that there may be more error introduced by the slight angle of the terminal flight path for that test and slightly lower velocity. This will be considered in detail when evaluating the results from the experimental series.

Orthogonal array results

The orthogonal array analysis is complicated slightly by the fact that the single 25.4 mm thick plate tests of every diameter stopped the projectile, while the rest did not. This means that no one continuous parameter can be used for evaluation in the method via standard means. We therefore make a slight adjustment to the method in that when evaluating the plate diameter and bolt torque parameters, only the tests from which an exit velocity is measured are used for effectiveness calculations. The results from the single plate tests will be evaluated separately, and connections will be made relating the single plate tests to the results from the level averages study. Additionally, a parameter called damage angle is used as a continuous parameter in this evaluation. This parameter is found by processing the CT images and determining the angle separating the little to no damage zone from the area of significant damage. The angle is determined by a visual inspection process of the CT images using the software package AVIZO and identifying the point of first far field and major delamination. The flat front face of the plate far from the disturbed location of penetration is used as the horizontal reference for the damage angle. The vertex is placed just before the main damage channel where the density of material drops significantly. The angle is then measured from this horizontal reference to the major delamination described previously. This process can involve some error as the scans are accurate to 55.7 um and a visual identification of the major delamination site is used, with total process error estimated at ± 0.05 degrees. This is not enough to impact the results of this study, and allows for the use of another quantifiable parameter for evaluation of results and provide value to the community. The 2.54 cm by 15.2 cm plate scan is shown in Fig. 2 as an example of the CT scan an angle identification. The average damage angle is shown to be 18.5 degrees and it is seen that the significant observed damage occurs above the line of the angle, while mostly consolidated and undamaged material is underneath it. This observation and pattern hold for all plates as will be seen in scans shown in future sections. The damage patterns lend themselves to this type of linear progression of damage from the impact location and is consistent with the observed tenting effect of Dyneema during high-speed impacts [9, 13, 14]. All images are therefore taken when the scan result is aligned with one of the fiber directions such that a 0° layer is parallel running left/right in plane and a 90° layer is perpendicular out of the plane.

Plate Spacing The results from the level average study for plate spacing is shown in Fig. 3. This clearly indicates that a single plate performs best, and that continuing to spread out the material while maintaining areal density decreases performance. Test 4 is included in the 2×12.7 mm category, but the trend of the two plate test performing better than the four plate tests is consistent when looking at the 25.4 cm diameter tests indicating a minimal impact on the conclusion of the analysis. Curiously, it does not appear that the 15.2 cm plates are as sensitive to the plate spacing, with the two and four plate configurations at that diameter behaving effectively the same. This claim is re-affirmed by the even closer matching delta v values for the two tests and the fact that the higher exit velocity of the pair also has the slightly higher input velocity. Additionally, the difference in bolt

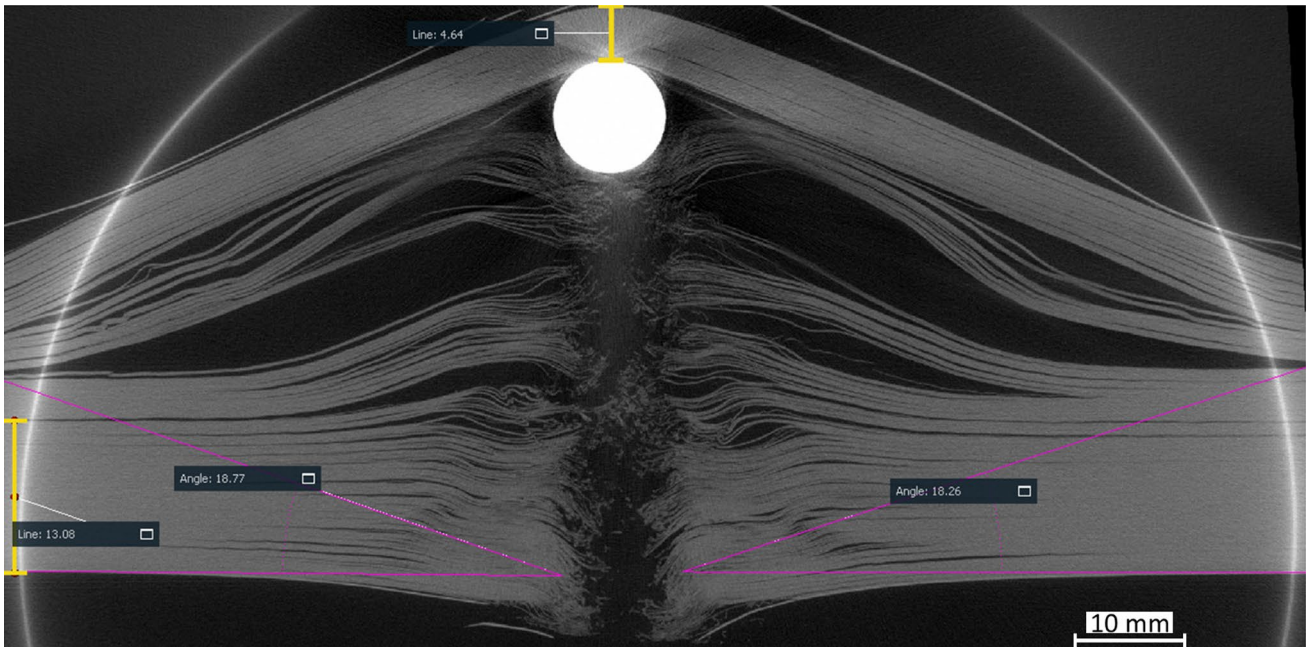

Fig. 2 CT scan of the 2.54 cm × 15.2 cm target after penetration. The damage angle is on average 18.5 degrees and there is 4.64 mm of un-penetrated plate ahead of the projectile. All lengths are in millimeters and angles are in degrees. The plate first suffers shear plug failure, followed by a transition zone (fiber snap back), before moving into a delamination dominated failure mode

torque for these tests could also contribute to the four plate configuration having a slightly better performance as will be discussed later. All of these effects are consistent with each other in the resulting conclusion.

When evaluating the damage angle, a clear trend exists linking a larger angle to thicker or more consolidated plates and indicating a relationship between damage angle and performance. The analysis from the damage angle is also consistent

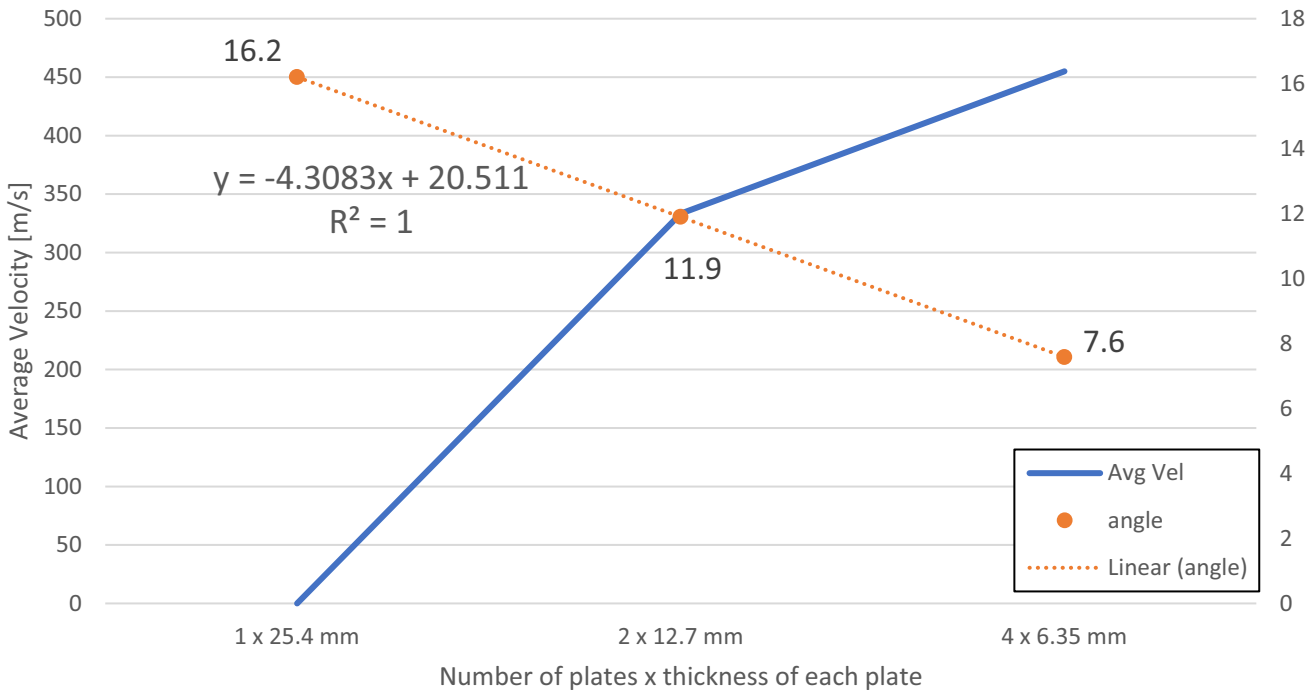

Fig. 3 Level average analysis for the plate spacing parameter, showing that a single consolidated plate performs best, followed by 2 12.7 mm plates, with 4 6.35 mm plates performing worst

with the exit velocity criteria which validates the use of damage angle for material performance. The CT scan results for the 20.3 cm diameter plates, shown in Fig. 4, illustrate the decrease in the damage angle with an increase in plate number. The highest average damage angle for a given diameter is always on the 1×25.4 mm test, followed by the 2×12.7 and finally the 4×6.35. For the 2 plate tests, the first plate always has a better damage angle compared to the second, with both plates being worse than the single plate tests. The second plate damage angle is also always greater than any damage angle for any plate from the 4 plate tests for a given diameter. These higher damage angles in the 2 plate tests help explain why the 2 plate tests perform better than the 4 plates when considering the exit velocity as an evaluation metric. To approximate this trend numerically, the damage angle can be predicted with the following equation:

$$damage\ angle = 20.511 - 4.3083\ (number\ of\ plates)$$

This equation has a strong resemblance to the experimentally collected data with an R squared value of 1 indicating not only an excellent fit, but also a strong linearity in the relationship between the number plates and damage angle.

Curiously, the third plate in the 4 plate stacks always has the greatest damage angle; 7.4, 9.3 and 11.7 degrees corresponding to the 25.4, 20.3, and 15.2 cm diameter cases. This increase in damage angle and therefore performance in a later plate is likely due to the slowing of the projectile and an interaction between the plates. The second plate is deforming and making contact with the third plate, pre-loading it before the actual penetration event, and the third plate is also similarly interacting with the final plate which provides some degree of reinforcement and therefore and increase in performance.

Plate Diameter Results for analyzing plate diameter are shown in Fig. 5 which indicate that performance decreases with an increase in plate diameter. Again, these values are calculated using only the non-zero exit velocities from the two and four plate tests. These results are however supported by the CT scans of the single plate tests which shows the same trend in amount of unpenetrated plate, as seen in Table 2 and Fig. 6, meaning that the smallest diameter plate had the best performance. This is consistent with the findings presented in Fig. 5. The slightly anomalous Test 4 is included in the 20.3 cm plate calculations, but qualitatively accounting for this would result in a slight increase in the average exit velocity for the 20.3 cm series which would not alter the conclusions of the analysis.

When analyzing the CT images and damage angle a similar trend is observed where the smallest diameter has the largest angle which can be seen in Fig. 6. Along with these values the distance from the front of the plate to the first major delamination, as noted by the yellow lines in the bottom left of each image of Fig. 6, also increase as the diameter decreases. Also of interest is the clear change in failure mechanism with the diameter. As the plate diameter is reduced there is significant cavitation, or creation of large pockets of empty space in the material, and large layer separation is generated. This leads to a larger back-face deformation and an increase in performance, which is counter to conventional methods when evaluating body armor which rank plates lower when the back-face deformation is larger [15, 16]. All three plates at the 25.4 mm thickness show significant fiber curling at the transition from shear plug failure to significant load in the fibers and fiber snap, which coincides with the depth of the first major delamination and is circled in red. To numerically quantify the damage angle as a function of plate diameter, a linear relationship is defined as:

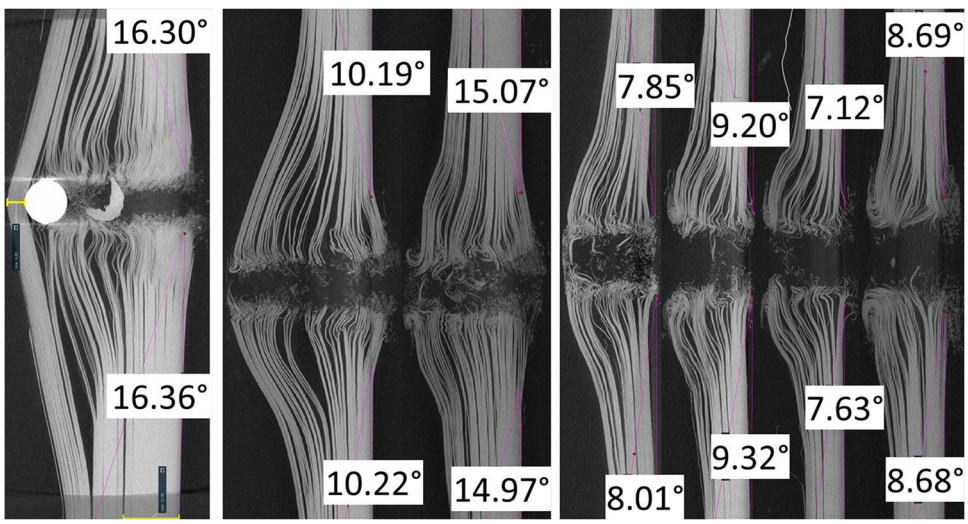

Fig. 4 The 1×25.4 mm, 2×12.7 mm, and 4×6.35 mm scan results for the 20.3 cm diameter plates where the projectile penetrates right to left and the damage angle measurements are in degrees. The trend of decreasing damage angle with an increase in the number of plates is consistent across all diameter classes

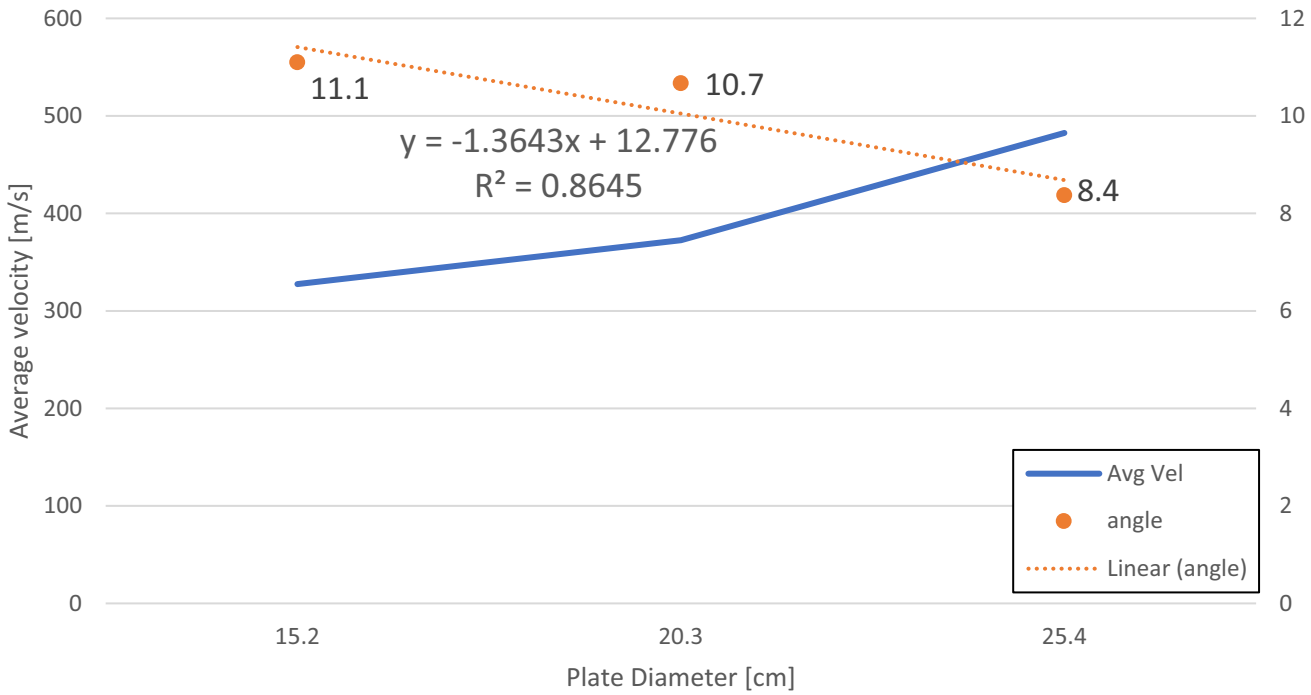

Fig. 5 Level average analysis for the plate diameter parameter, showing a decrease in performance with an increase in diameter. This analysis is supported by the data from the single 25.4 mm plate results which are evaluated based on amount of unpenetrated plate ahead of the projectile

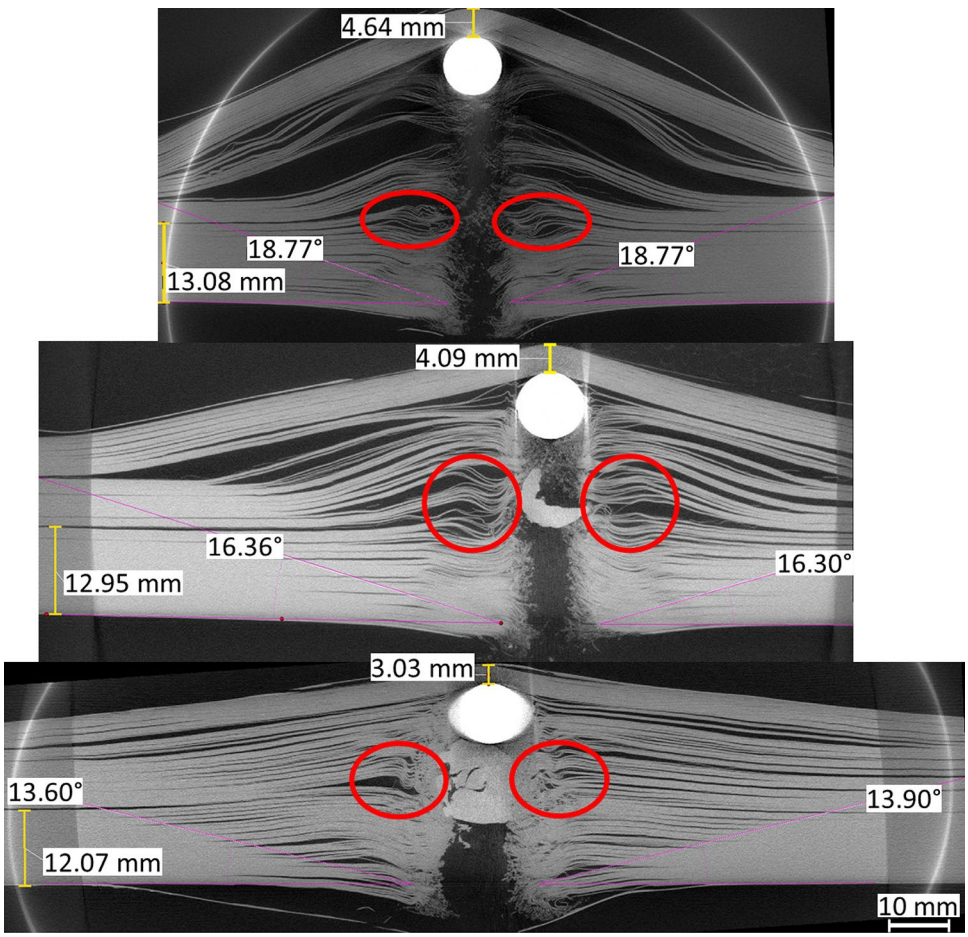

Fig. 6 The 15.2 cm plate (top), 20.3 cm plate (middle) and 25.4 cm plate (bottom). The measured damage angle in degrees, amount of unpenetrated plate ahead of the projectile in millimeters, and distance from the front of the plate to the first minor far field delamination plane in millimeters all increase as the plate diameter decreases. The fiber snap back region in each plate which is circled in red

$$damage\ angle = 12.776 - 1.3643\ (plate\ diameter\ in\ cm)$$

This equation on its own does a fair job of capturing the trend with an R squared value of 0.86. Logically, there must be a point of diminishing returns on either extreme for diameter where at a very large diameter the damage angle approaches a fixed value and at some smaller diameter the angle (and performance) must decrease as there will be too little material to effectively absorb and / or dissipate the energy from the impact event. However, over this range of diameters the fit of this equation is applicable and shows a good correlation to collected data.

Bolt Torque Bolt torque analysis results are shown in Fig. 7. The analysis seems to indicate that the material would perform better at either very high or very low bolt torques, but the low torque spec of 2.7 N-m contains the data point from the slightly anomalous test 4 which could be decreasing the average exit velocity in this analysis. Further, evaluating the single 25.4 mm thick test shots shows that the medium torque parameter behaves best followed by the high spec with the low torque performing the worst. When considering these results together, we conclude that the clamping pressure does not have a strong trend although that it appears as though higher bolt torques may be beneficial. This is likely caused by the compressive preload of the higher bolt torques closing any meso or microscopic voids in the material thus increasing the overall strength by facilitating better stress wave transmission through the entire target.

The trendline in damage angle vs bolt torque is nearly flat as shown in Fig. 7, and the R squared value is less than 0.01. This finding again confirms that the bolt torque has minimal effect on impact tests of this type. Additionally, there is nothing in the CT scans of the similar bolt torque level tests that consistently links them across tests further confirming the assertion stated previously.

CT Scan Analysis and Failure Mechanism Discussion

All targets display a delamination / damage angle which shows that the damage grows in plane as the projectile penetrates. The damage angle was discussed in the analysis of "Orthogonal array results" section, so the focus of this section is to examine the other failure mechanisms observed in the CT scans. For the purpose of brevity, the failure mechanisms discussion is organized by the plate spacing parameter as that had the strongest trend when looking at both the residual projectile velocity and the damage angle as evaluation parameters. On the whole, increased delamination based cavitation is the primary mechanism that leads to increased performance, as across all three plate spacing categories those with increased performance displayed increased cavity generation. This effect is not as strong in the 4×6.35 mm

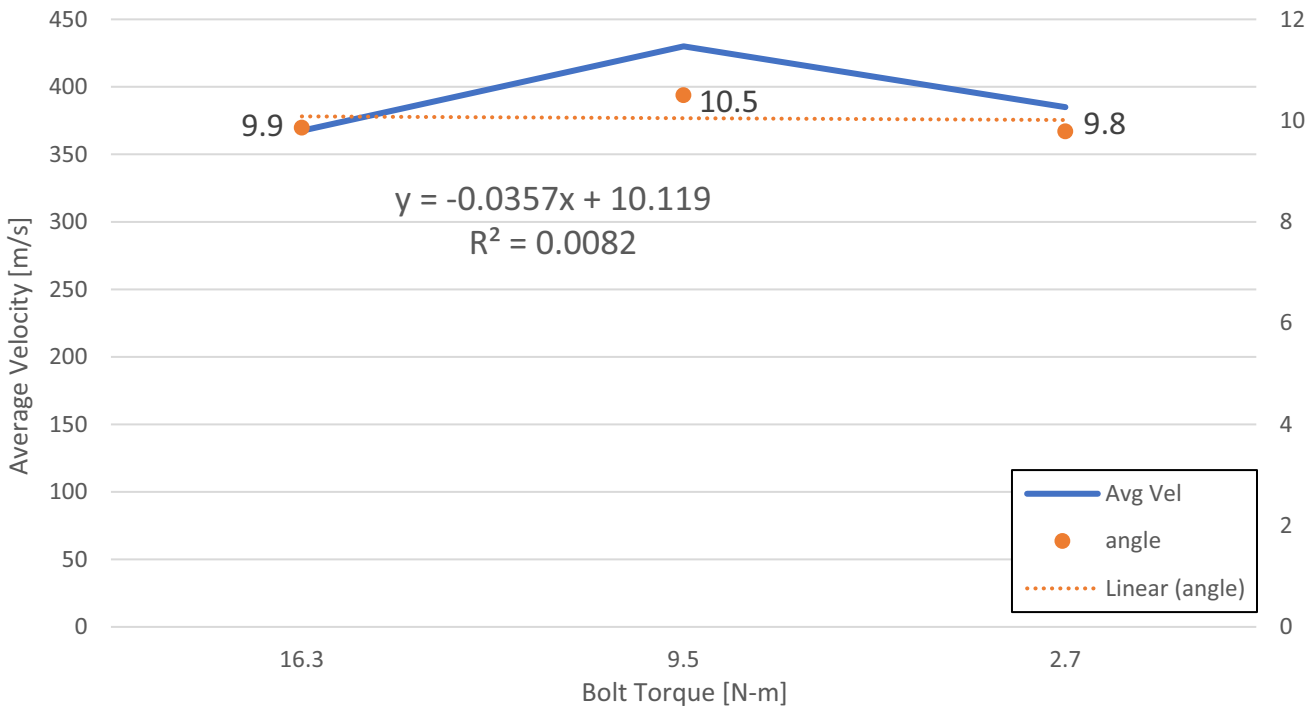

Fig. 7 Level average analysis for the bolt torque parameter. This analysis does not include the results from the single 25.4 mm thick tests as was discussed earlier in "Orthogonal array results" section

plate tests which is consistent with the analysis of the plate spacing parameter in "Plate Spacing" section.

25.4 mm thick plates

The scans of the 25.4 mm thick targets show a considerable change in failure mechanism and are displayed in Fig. 6. While the amount of un-penetrated plate remaining increases with a decreasing diameter, the total back face deformation appears to have the inverse relationship. This likely leads to the apparent increase in performance for smaller diameter plates as more delamination occurs and more load is taken up in the fibers due to the indirect tensile mechanism having more of an opportunity to take effect. Additionally, the larger diameter 25.4 cm target does not have as clear of a division between shear plug and delamination zones.

The overall trend among the tests in Fig. 6 indicates that peak back face deformation is in fact linked to the damage angle of the target, and that an increase in either is indicative of increased performance when evaluating based upon amount of un-penetrated plate remaining. This is again consistent with the discussion in "Calibration Tests" section in which the 25.4 mm × 15.2 cm target was able to capture a 1170 m/s projectile, which is 70 m/s faster than the penetration speed of a 20.3 cm diameter target. After the shear plug failure zone, which is the initial damage zone with little to no delaminations far from the penetration channel, all of the targets show a significant curl in the fibers. This curl, referred to as fiber snap back, is a key internal failure feature and exists at the transition from shear plug to delamination damage dominated failure. This transition occurs deeper into the targets as the diameter decreases as noted by the depth of the first minor far field delamination shown in the lower left of the images in Fig. 6. The variation is only one millimeter in depth, and the difference between the 15.2 cm and 20.3 cm diameter plates is about 0.1 mm inferring that this value is approaching a constant value at the 15.2 cm diameter size.

12.7 mm thick plates

The 2 plate test scans are shown in Fig. 8. Test 4, which was the 2 plate test of 20.3 cm diameter, is shown in the middle and at a first glance appears to perform about the same for plate one of the stack compared to the 15.2 cm diameter. This can be accounted for by considering the slightly slower impact velocity of the 20.3 cm test and the minor impact of a small piece of sabot on the first plate of the 15.2 cm × 2 plate test which is on the left of Fig. 8. The second plates of this series tells a better story, with a clear improvement in the damage angle for the smaller diameter plates. The back face deformation of the plates does increase as the diameter decreases, which is consistent with the single 25.4 mm thick plates shown in Fig. 6. With this increase in back face deformation comes an increase in delamination based cavity generation. It is this significant delamination which absorbs the energy of the impact and is indicative of the fibers sustaining more of the load and deforming more before finally breaking. Fiber snap back occurs in the second plate of each test, with the first plate being fully punctured and exhibiting solely shear plug or fiber breakage type failure.

6.35 mm thick plates

Following the trends from the 25.4 mm plate to the 12.7 mm plates, the 6.35 mm plates have lower damage angles and less backface deformation, as seen in Fig. 9, which is consistent with the analysis provided in "Plate Spacing"

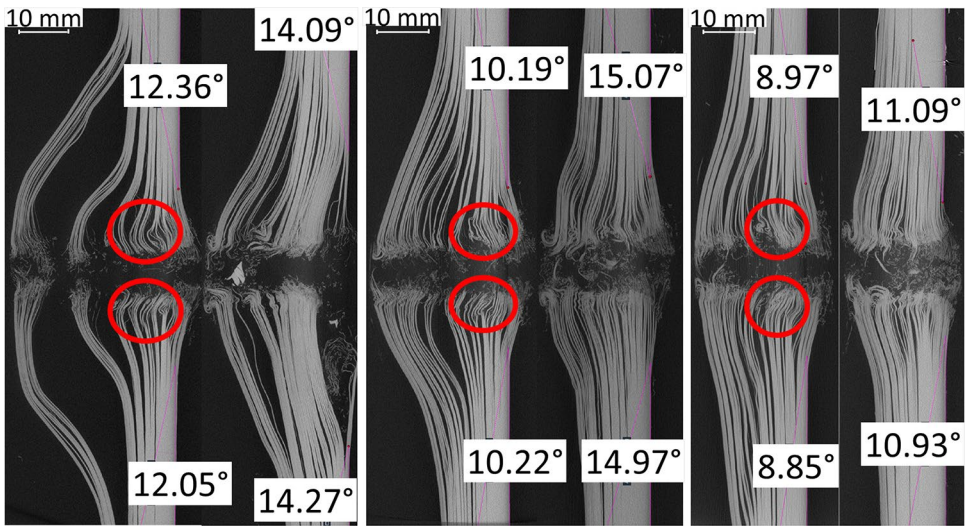

Fig. 8 The 2 plate test scans for the 15.2 cm diameter (left), 20.3 cm diameter (middle), and 25.4 cm diameter (right). The projectile penetrates from right to left and the measurements are in degrees. Fiber snap back zones are identified in the second of each series and are circled in red

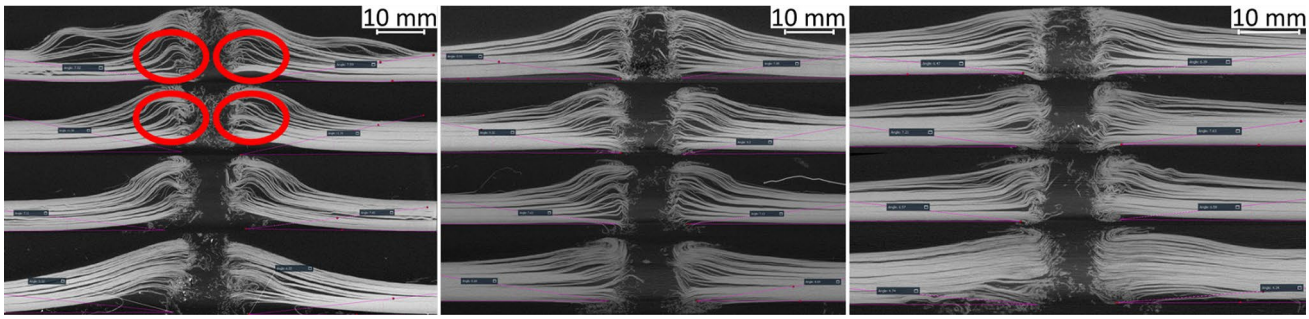

Fig. 9 The four plate tests of the 15.2 cm diameter (left) 20.3 cm diameter (middle) and 25.4 cm diameter (right). Only the 15.2 cm diameter test displayed significant fiber snap back, circled in red, and delamination based cavitation beyond the circled regions

section. Additionally, the targets of the three different diameters do not show as definitive of a fiber snapback zone, with only the 15.2 cm diameter set displaying a clear region in both the third and fourth plates. This lack of fiber snap back, which in the larger plates marked the transition from shear plug dominated to delamination dominated damage zones, explains why the four plate stacks did not perform as well as the thicker counterparts for the larger diameter sizes.

Damage Theory Discussion

A trend in the failure mechanics of the plates are observed across the diameter and the plate spacing parameters. Bolt torque was found not to be a significant variable in these experiments and is therefore not considered. The plates begin with a shear plug dominated zone. In this region, the fibers of the composite are not strong enough to significantly deform before puncture. The layer is quickly perforated before much of the energy can be deposited into the surrounding material in the plate. Eventually the projectile has lost enough speed and energy to this process that the fibers begin to hold load and transfer it to the surrounding material, resulting in some stretching of the fibers before they are broken and transfer of energy to the surrounding material. This loading of the fibers before they are punctured creates the fiber snap back region which is observed at the end of the shear plug failure zone. These fibers are stretched, storing energy in their deformation before they break, which results in the curl as the residual stress is release so quickly that it effectively pulls the fibers back towards the edges of the plate. As the projectile continues to penetrate, the speed continues to decrease so the fibers do a better job at transferring the load to the surrounding material resulting in more delamination and delamination occurring farther from the projectile. This overall process of shear plug to fiber snap back to full delamination can be seen clearly in Fig. 6 as an example and is why the damage zone can be represented by an angle. The delaminations can reach farther towards the edges as the projectile losses energy which is driven by the increasing ability of the fibers to carry load.

From these scans we propose a theory for the performance of the material in these tests. Primarily the stiffness of the plates relative to each other is of paramount importance. The smaller diameter plates are fundamentally stiffer than the larger diameter ones in an edge supported configuration such as that examined in this study, meaning that the larger diameter plates flex or bend more during the penetration event as the plates attempt to catch the projectile. As a result of this higher flex at higher diameters, the plate is more prone to increased delaminations as the overall movement of the plate is increased. This results in a shallower damage angle as more of the plate delaminates with less backface deformation or cavity generation. The smaller diameter plates by contrast do not flex or bend to the same degree. This lack of bending encourages more of a pure shear plug failure in the initial penetration, preventing additional delaminations in this shear zone and causing a larger damage angle. This theory is also supported by the increase in the distance from the front of the 25.4 mm plates to the site of the first far field minor delamination which is consistent with the proposed mechanism of damage. The decreased performance and decreased damage angle is also seen when reducing the thickness of the plates. These plates will also have a reduced stiffness as a result, which is again a consistent point with proposed analysis. This theory explains why the bolt torque parameter had a minimal impact on the testing parameters. This torque does not significantly change the stiffness of the plates, especially when compared to parameters such as diameter and thickness which have clear and fundamental links to the stiffness of materials.

To reinforce the concepts described above regarding the importance of stiffness and rigidity to the performance of the material, we present an analytical model for the deflection of a circular plate under a centrally located point load. The plate dimensions are defined by the radius r and thickness t. The derivation assumes clamped edge boundary conditions subject to a point load q, and a homogenous material of modulus E and poisson's ratio ν. This equation, equation (1), is given below [17].

$$maximum\ deflection\ = \frac{q\ r^2\ [12(-\nu)]}{16\pi\ E\ t^3} \tag{1}$$

While this equation is for elastic deformation of an isotropic homogeneous material, there are trends that can be observed from it that help illustrate the influence of stiffness. The maximum deflection is proportional to r^2 and t^{-3}, meaning as the radius decreases and the thickness increases, the maximum deflection for a fixed load is less indicating a stiffer system. Conversely, as the radius increases and the thickness decreases, the maximum deflection for a fixed load will increase. The trends observed in this model are consistent with the claim of increased stiffness leading to increased performance as stated above.

Conclusion

The method of orthogonal arrays was used to design a set of impact experiments to evaluate the performance of UHMWPE hard composites, and high resolution CT scanning technology was used to aid in analysis and damage mechanism identification while not obstructing or otherwise damaging the site by physically cross sectioning it. From this analysis, it is clear that the plate spacing parameter is the most critical amongst those investigated and that bolt torque had little impact on the effectiveness of the tests. The 25.4 mm consolidated plates all successfully captured a 9.5 mm diameter steel projectile traveling at approximately 1030 m/s. The two plate stacks consisting of two 12.7 mm diameter plates performed better than the 4 plate × 6.35 mm thickness per plate tests showing the effect of an air gap while maintaining the effective areal density of material. Plate diameter also proved to be an effective parameter in the design of armor packages, with a smaller diameter performing better than a larger one. This result likely speaks to the impact of the boundary condition on material response, as the CT scans of these targets shows how the smaller diameter targets have a more prominent delamination driven cavity generation compared to the larger diameter plates. Additionally, the damage angle measure from the tests was found to have a strong correlation to performance, with an R squared value of 1 for the plate spacing parameter fit and a 0.86 for the plate diameter which mean a strong correlation between these parameters and the damage angle. Additional back face deformation correlates to an increase in performance, which is attributed to additional energy dissipation through material movement and the creation of free surfaces and air cavities via delamination.

Appendix A: Orthogonal Arrays and Parameter Details [18]

The method of orthogonal arrays is used in the design of the experiments and analyzing the results. Consider a basic example of an experiment involving four parameters on a continuous scale. As testing the entire continuum of options is impossible, levels of each parameter are selected. In a testing space where there are four parameters and three levels of each parameter, testing all possible combinations yields $3^4 = 81$ tests. If one uses an orthogonal array the total number of tests is only nine. The effect is even more pronounced as the numbers of parameters and levels grows. For experiments with five parameters and five levels for each, full factorial testing requires 3,125 tests while the orthogonal array for this type of experiment consists of only 25 tests. This testing methodology is especially useful when restricted by facility access time, budget, availability of material, or some other external factor that reduces the number of tests possible in an experimental series.

An analysis technique called level averages is used to make the data useful for design. Level averaging is where an average over all data points X are taken for a given level of a parameter. For example, the level average for parameter "c" at level 1 is (X1 + X6 + X8)/3 = Xc1. Similar calculations can be done to find the remaining 11 level averages. These values are then plotted against the values of the levels themselves, and these plots are used to identify the best performing level. As can be seen in Fig. 10

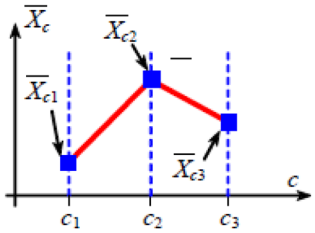

Fig. 10 Level averages plotted on the y axis vs. levels of the parameter on the x axis

the level c2 is a local maximum, meaning it is the best performing level of that parameter if a maximum value of the evaluation criteria is desired. As will be seen later, for this series of tests minimum values are desired as exit velocity of the penetrator is the main metric. It should be noted that in ideal conditions at least three levels of each parameter should be tested to ensure the possibility of local minima and maxima in the plots.

Plate Diameter

The levels for this parameter are 15.2 cm, 20.3 cm, and 25.4 cm diameters. This could identify a critical diameter below or above which there is a significant reduction in stopping capability. The interaction will also inform some of the interaction between the plate and the support structure. The smaller plates will be able to transfer the load to the supports faster as the travel distance from the point of impact to the support is reduced. Conversely, there is less material and potentially less volume to create delamination surfaces to dissipate additional energy. These diameter levels were selected as 20.3 cm and 25.4 cm are common dimensions for plates in use as inserts for ballistic vests, and 15.2 cm was selected because it represents the smallest typical commercial plate dimension. 25.4 cm will most closely approximate an "infinite" plate boundary condition, while the smallest diameter should see some interaction with the support fixture, described in "Test Fixture Design" section and Appendix B.

Plate Spacing

It has been shown that the effectiveness of Dyneema® increases if it is allowed to bulge on its blackface [19]. This parameter will investigate this effect of self-restriction for deformation due to excess material versus the ability of the material to transfer the load quickly via stress waves to the entire plate, which has not been widely addressed to date. The aim is to ascertain how the act of spreading out the Dyneema® will impact its performance while the total amount of material in each configuration, otherwise known as areal density, is maintained. This is achieved by testing a single plate 25.4 mm thick, two plates measuring 12.7 mm thick separated by a 1.8 cm gap, and four 6.35 mm thick plates separated by a 9.5 mm gap. The change in gap size was done to allow the thicker material more time and room to deform before the full penetration event and before interacting with the next plate, due to the increased stopping potential from increased thickness of the individual plate. This parameter was also informed by results from previous exploratory experiments. It may be of interest to examine the impact of varying the air gap thickness on stopping power in future experiments. For the purpose of these experiments however, the air gaps are kept fixed.

Bolt Torque

This parameter refers to torquing down the bolts in the plate assembly to 3 different levels being: low, 2.7 N-m, intermediate, 9.5 N-m, and high 16.3 N-m. Low is just enough pressure to keep the plates from sliding due to gravity and is a quantified metric for hand tight. The high spec generates a pressure such that the motion of the clamped section of plate is minimized, ideally fixed, while also not permanently deforming the plates. Low should represent close to a free edge boundary condition, high will replicate a fixed boundary condition, and intermediate will be half way between the two. This will provide more data on a different kind of boundary condition from that in plate diameter, while also providing data for approximate free and fixed boundary conditions radially at the clamp interface.

Appendix B: Test Fixture Drawings

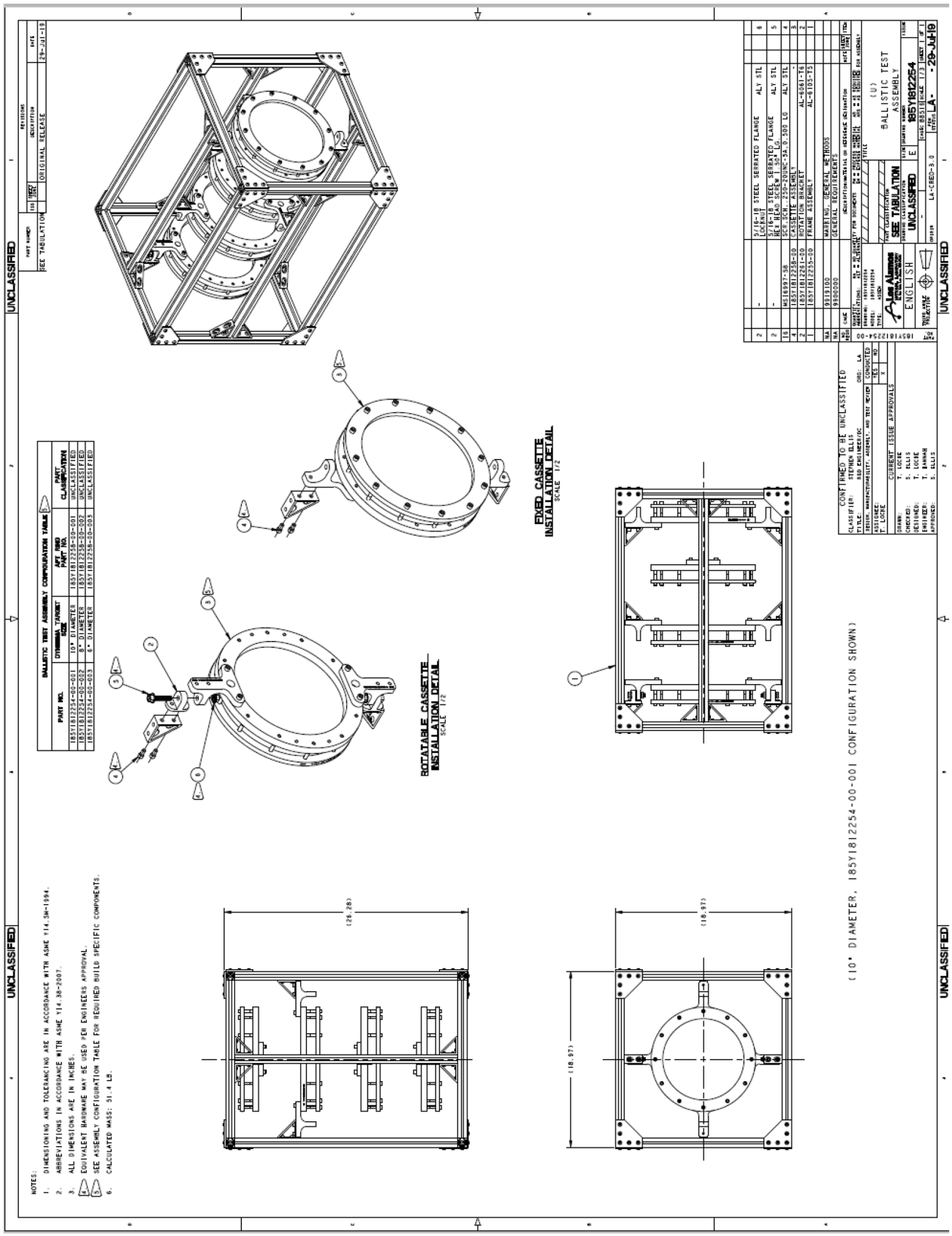

UNCLASSIFIED

NOTES:

1. DIMENSIONING AND TOLERANCING ARE IN ACCORDANCE WITH ASME Y14.5M-1994.
2. ABBREVIATIONS IN ACCORDANCE WITH ASME Y14.38-2007.
3. ALL DIMENSIONS ARE IN INCHES.
4. REMOVE ALL BURRS AND BREAK SHARP EDGES TO .020 MAXIMUM.
5. COUNTERSINK TAPPED HOLES TO MAJOR DIAMETER.
6. BREAK SHARP EDGES TO .005 MAXIMUM ON ALL CLEARANCE HOLES.
7. ALL INSIDE CORNERS TO BE R .010 MAX.
8. MARK PART IDENTIFICATION NUMBER, REVISION LETTER, CLASSIFICATION, PER 9919100 CLASS A-I-A APPROXIMATELY WHERE SHOWN IN APPROXIMATELY .125 INCH HIGH LEGIBLE GOTHIC/LEROY CHARACTERS.
9. CALCULATED MASS: 2.4 lbs.

PART NUMBER	REVISIONS			
	ISS	SHEET ZONE	DESCRIPTION	DATE
SEE TABULATION	A		ORIGINAL ISSUE	25-Jul-19

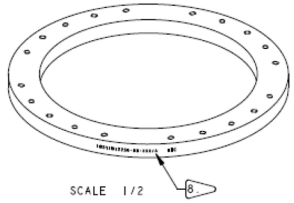

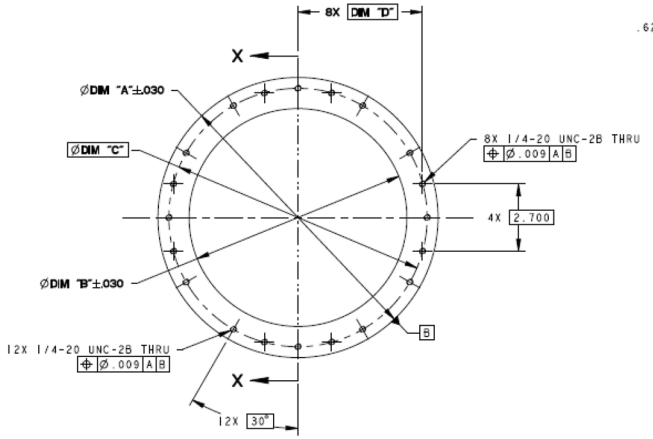

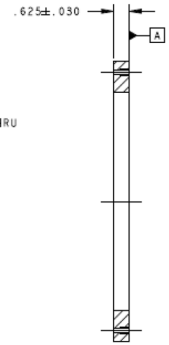

SECTION X-X

AFT RING CONFIGURATION TABLE						
PART NO.	DYNEEMA TARGET SIZE	DIM "A" DIAMETER	DIM "B" DIAMETER	DIM "C" DIAMETER	DIM "D" DIAMETER	PART CLASSIFICATION
185Y1812256-00-001	10" DIAMETER	11.250	8.750	10.375	5.000	UNCLASSIFIED
185Y1812256-00-002	8" DIAMETER	9.250	6.750	8.375	4.000	UNCLASSIFIED
185Y1812256-00-003	6" DIAMETER	7.250	4.750	6.375	3.000	UNCLASSIFIED

CONFIRMED TO BE UNCLASSIFIED
CLASSIFIER: STEPHEN ELLIS
TITLE: R&D ENGINEER/DC ORG: LA

DESIGN, MANUFACTURABILITY, ASSEMBLY, AND TEST REVIEW	CONDUCTED	
ASSIGNEE:	YES	NO
T. LOCKE	X	

CURRENT ISSUE APPROVALS

DRAWN:	T. LOCKE
CHECKED:	S. ELLIS
DESIGNED:	T. LOCKE
ENGINEER:	T. HANNAH
APPROVED:	S. ELLIS

NO. REQD	PART/CONTROL NO	DESCRIPTION/MATERIAL OR REFERENCE DESIGNATION	NOTE	SHEET ZONE	ITEM
AR	-	AMS-QQ-A-200/8 OR AMS-QQ-A-250/11 AL-6061-T6			
NA	9919100	MARKING, GENERAL METHODS			
NA	9900000	GENERAL REQUIREMENTS			

QUANTITY ABBREVIATIONS: NA = NO QUANTITY FOR DOCUMENTS PM = PROCESS MATERIAL AR = AS REQUIRED EM = EXPENSE MATERIAL ARS = AS REQUIRED FOR ASSEMBLY

DRAWING: 185Y1812256
MODEL: 185Y1812256
TYPE: PART

Los Alamos NATIONAL LABORATORY

ENGLISH

THIRD ANGLE PROJECTION

PART NO. 185Y1812256-00

TITLE
(U)
AFT
RING

PART CLASSIFICATION: SEE TABULATION

DRAWING CLASSIFICATION: UNCLASSIFIED

SIZE	DRAWING NUMBER	ISSUE
D	185Y1812256	A

CAGEC 88516 SCALE 1/2 SHEET 1 OF 1

ORIGIN LA-CREO-2.0 TDM STATUS LA - WIP - 25-Jul-19

UNCLASSIFIED

UNCLASSIFIED

NOTES:

1. DIMENSIONING AND TOLERANCING ARE IN ACCORDANCE WITH ASME Y14.5M-1994.
2. ABBREVIATIONS IN ACCORDANCE WITH ASME Y14.38-2007.
3. ALL DIMENSIONS ARE IN INCHES.
4. REMOVE ALL BURRS AND BREAK SHARP EDGES TO .020 MAXIMUM.
5. COUNTERSINK TAPPED HOLES TO MAJOR DIAMETER.
6. BREAK SHARP EDGES TO .005 MAXIMUM ON ALL CLEARANCE HOLES.
7. ALL INSIDE CORNERS TO BE R .010 MAX.
8. MARK PART IDENTIFICATION NUMBER, REVISION LETTER, CLASSIFICATION, PER 9919100 CLASS A-1-A APPROXIMATELY WHERE SHOWN IN APPROXIMATELY .125 INCH HIGH LEGIBLE GOTHIC/LEROY CHARACTERS.
9. CALCULATED MASS: 1.4 lbs.

PART NUMBER	REVISIONS			
	ISS	SHEET ZONE	DESCRIPTION	DATE
SEE TABULATION	A		ORIGINAL ISSUE	18-Jul-19

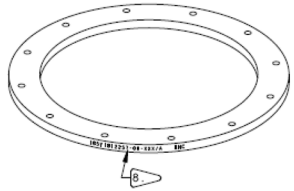

SCALE 1/2

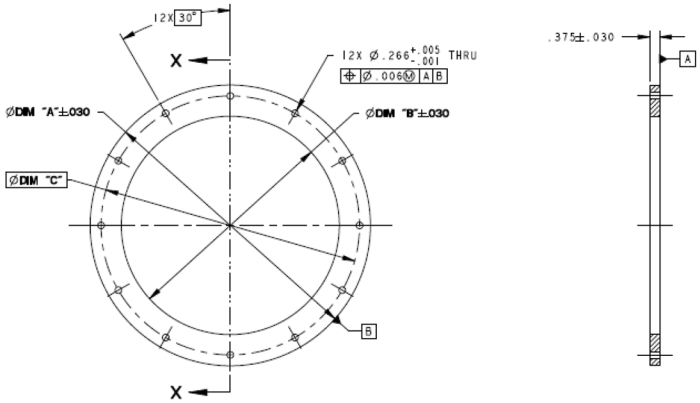

SECTION X-X

FORWARD RING CONFIGURATION TABLE					
PART NO.	DYNEEMA TARGET SIZE	DIM "A" DIAMETER	DIM "B" DIAMETER	DIM "C" DIAMETER	PART CLASSIFICATION
185Y1812257-00-001	10" DIAMETER	11.250	8.750	10.375	UNCLASSIFIED
185Y1812257-00-002	8" DIAMETER	9.250	6.750	8.375	UNCLASSIFIED
185Y1812257-00-003	6" DIAMETER	7.250	4.750	6.375	UNCLASSIFIED

CONFIRMED TO BE UNCLASSIFIED
CLASSIFIER: STEPHEN ELLIS
TITLE: R&D ENGINEER/DC ORG: LA

DESIGN, MANUFACTURABILITY, ASSEMBLY, AND TEST REVIEW	CONDUCTED	
ASSIGNEE:	YES	NO
T. LOCKE	X	

CURRENT ISSUE APPROVALS

DRAWN:	T. LOCKE
CHECKED:	S. ELLIS
DESIGNED:	T. LOCKE
ENGINEER:	T. HANNAH
APPROVED:	S. ELLIS

NO. REQD	PART/CONTROL NO	DESCRIPTION/MATERIAL OR REFERENCE DESIGNATION	NOTE	SHEET ZONE	ITEM
AR	-	AMS-QQ-A-200/8 OR AMS-QQ-A-250/11 AL-6061-T6			
NA	9919100	MARKING, GENERAL METHODS			
NA	9900000	GENERAL REQUIREMENTS			

QUANTITY ABBREVIATIONS: NA = NO QUANTITY FOR DOCUMENTS PM = PROCESS MATERIAL AR = AS REQUIRED
ALT = ALTERNATE EM = EXPENSE MATERIAL ARS = AS REQUIRED FOR ASSEMBLY

DRAWING: 185Y1812257
MODEL: 185Y1812257
TYPE: PART

Los Alamos NATIONAL LABORATORY

ENGLISH

THIRD ANGLE PROJECTION

PART NO. 185Y1812257-00

TITLE
(U)
FORWARD
RING

PART CLASSIFICATION
SEE TABULATION

DRAWING CLASSIFICATION
UNCLASSIFIED

SIZE	DRAWING NUMBER	ISSUE
D	185Y1812257	A

CAGEC 88516 SCALE 1/2 SHEET 1 OF 1

ORIGIN LA-CREO-2.0 TDM STATUS LA - WIP - 18-Jul-19

UNCLASSIFIED

Acknowledgements We would first and foremost like to thank Los Alamos National Laboratory (LANL) for their funding and support of this work. Additionally, we would like to thank M-6 at LANL for support of equipment and facilities when conducting the experiments. We would also like to thank the Materials Characterization Lab at Penn State for support when conducting the CT scans post-test.

Author Contribution All authors contributed to the study conception and design of the work presented.

Funding Los Alamos National Laboratory.

Declarations

Conflicts of Interest The authors declare no conflicts of interest under this work.

References

1. Jacobs MJN, Dingenen JLJV (2001) Ballistic protection mechanisms in personal armour. J Mater Sci 36(13):3137–3142. https://doi.org/10.1023/A:1017922000090
2. Levi-Sasson A et al (2014) Experimental determination of linear and nonlinear mechanical properties of laminated soft composite material system. Compos B Eng 57:96–104. https://doi.org/10.1016/j.compositesb.2013.09.043
3. Pundhir N, Pathak H, Zafar S (2021) Ballistic impact performance of ultra-high molecular weight polyethylene (UHMWPE) composite armour. Sādhanā 46(4):194. https://doi.org/10.1007/s12046-021-01730-0
4. Li Y, Fan H, Gao X-L (2022) Ballistic helmets: Recent advances in materials, protection mechanisms, performance, and head injury mitigation. Compos B Eng 238:109890. https://doi.org/10.1016/j.compositesb.2022.109890
5. Vargas-Gonzalez LR, Walsh SM, Gurganus JC (2011) Examining the relationship between ballistic and structural properties of lightweight thermoplastic unidirectional composite laminates. Army Res Lab, ARL-RP-0329
6. Mines RAW, Roach AM, Jones N (1999) High velocity perforation behaviour of polymer composite laminates. Int J Impact Eng 22(6):561–588. https://doi.org/10.1016/S0734-743X(99)00019-6
7. Nguyen LH, Ryan S, Cimpoeru SJ, Mouritz AP, Orifici AC (2015) The effect of target thickness on the ballistic performance of ultra high molecular weight polyethylene composite. Int J Impact Eng 75:174–183. https://doi.org/10.1016/j.ijimpeng.2014.07.008
8. Qu K, Wu C, Liu J, Yao Y, Deng Y, Yi C (2020) Ballistic performance of multi-layered aluminium and UHMWPE fibre laminate targets subjected to hypervelocity impact by tungsten alloy ball. Compos Struct 253:112785. https://doi.org/10.1016/j.compstruct.2020.112785
9. Zhang TG, Satapathy SS, Vargas-Gonzalez LR, Walsh SM (2015) Ballistic impact response of Ultra-High-Molecular-Weight Polyethylene (UHMWPE). Compos Struct 133:191–201. https://doi.org/10.1016/j.compstruct.2015.06.081
10. Taguchi G, EA Elsayed, Hsiang TC (1988) Good Hardcover. Quality Engineering in Production Systems (Mcgraw Hill Series in Industrial Engineering and Management Science). Ergodebooks. Available: https://www.abebooks.com/9780070628304/Quality-Engineering-Production-Systems-Mcgraw-0070628300/plp. Accessed 13 Jun 2023
11. Davim JP (2003) Design of optimisation of cutting parameters for turning metal matrix composites based on the orthogonal arrays. J Mater Process Technol 132(1):340–344. https://doi.org/10.1016/S0924-0136(02)00946-9
12. Shenoy Heckadka S et al (2022) Investigation of the mechanical properties of flax/jute/UHMWPE reinforced melamine formaldehyde composites using cone beam computed tomography. J Nat Fibers 19(15):12280–12294. https://doi.org/10.1080/15440478.2022.2054898
13. Smith JC, McCrackin FL, Schiefer HF, Stone WK, Towne KM (1956) Stress-strain relationships in yarns subjected to rapid impact loading. Part IV: transverse impact tests. Text Res J 26(11):821–828. https://doi.org/10.1177/004051755602601101
14. Morrison BW. Investigation of Ultra High Molecular Weight Polyethylene (UHMWPE) textile backing systems integrated with ceramic sphere body armor systems. Defense Tech Inform Center
15. DoD Testing Requirements of Body Armor, Report No. D-2009-047 (Project No. D2008-D000JA-0263.000) (2009). Available: https://media.defense.gov/2009/Jan/29/2001712184/-1/-1/1/09-047.pdf. Accessed 12 Jun 2023
16. Ballistic Resistance of Body Armor NIJ Standard-0101.06 (2008) National Institute of Justice. Available: https://nij.ojp.gov/library/publications/ballistic-resistance-body-armor-nij-standard-010106. Accessed 12 Jun 2023
17. Gujar PS, Ladhane KB (2015) Bending analysis of simply supported and clamped circular plate. Int J Civ Eng 2(5)
18. Cimbala J (2009) Experimental design. Penn State University
19. O'Masta MR (2014) Mechanisms of dynamic deformation and failure in ultrahigh molecular weight polyethylene fiber-polymer matrix composites. University of Virginia. Available: https://libraetd.lib.virginia.edu/downloads/2j62s5266?filename=OMasta_Dissertation_Submitted_to_Libra.pdf. Accessed 11 Feb 2020